Zeitschrift für Kristallographie 206, 213–231 (1993)
 – 0044-2968/93 $ 3.00+0.00

Ferroelastic transformation and crystal structure of Ba-diluted lead phosphate, $(Pb_{1-x}Ba_x)_3(PO_4)_2$

J. Hensler[1], H. Boysen[2], U. Bismayer[1] and T. Vogt[3]

[1] Institut für Mineralogie und SFB 173, Universität Hannover, Welfengarten 1, D-30167 Hannover, FRG
[2] Institut für Kristallographie der Universität München, Theresienstr. 41, D-80333 München, FRG
[3] Institut Laue-Langevin, BP 156X, 38042 Grenoble, France

Herrn Professor Siegfried Haussühl zum 65. Geburtstag gewidmet

Received June 18, 1992; accepted November 13, 1992

Ferroelastic transformation / Crystal structure / Ba-dilution / Lead barium phosphate / Neutron powder diffraction

Abstract. Frozen-in order parameter fluctuations and the spread of the ferroelastic transition temperature over a wide temperature range are found in strongly barium-diluted lead phosphate crystals, $(Pb_{1-x}Ba_x)_3(PO_4)_2$. For x-values near 0.09 the phase boundary of the transformation $R\bar{3}m \rightarrow C2/c$ in the phase diagram lead phosphate-barium phosphate approaches $T_c = 0$ K. Small Ba-inhomogeneities corresponding to order parameter fluctuations lead to the coexistence of ferroelastic and paraelastic phases. The superposition of static monoclinic and rhombohedral signals are analyzed by neutron powder diffraction. The crystal structure of a sample with barium content $x = 0.08$ is refined for 8 K, 300 K and 700 K using the Rietveld technique. The evolution of the structural deformation on a local and a macroscopic length scale is studied using spectroscopic, X-ray and optical birefringence methods. In a $(Pb_{0.92}Ba_{0.08})_3(PO_4)_2$ powder sample the short range monoclinic deformation vanishes above 700 K.

Introduction

Lead phosphate is an improper ferroelastic which forms mixed crystals with barium phosphate. The crystal structure of $Pb_3(PO_4)_2$ was first determined by Keppler (1970) and has been reinvestigated by Guimaraes (1979).

The structure of the paraelastic high-temperature phase of lead phosphate with space group $R\bar{3}m$ (see also Fig. 8) is characterised by P-atoms tetrahedrally coordinated by oxygen atoms and lead atoms which occupy two large cation sites. Pb(1) with Wyckoff position *a* is twelvefold coordinated by oxygen neighbours, Pb(2) in *c*-sites is coordinated by ten oxygen atoms. The structure consists of interconnected chains PO_4-Pb(2)-Pb(1)-Pb(2)-PO_4 parallel to the threefold inversion axis. The stepwise transition from the para- to ferrophase $C2/c$ has been described by a three-states Potts model including displacive and order-disorder characteristics (Salje, Devarajan, 1981). Critical points are three symmetry equivalent L-points on the surface of the rhombohedral Brillouin zone which transform to the origin of the Brillouin zone of the monoclinic phase during the symmetry reduction. There are three order parameter components with two different critical temperatures. In $Pb_3(PO_4)_2$ one component shows a critical behaviour near 560 K corresponding to small Pb-displacements perpendicular to the threefold inversion axis. Below 560 K a flip rotation around this axis is thermally activated. At the ferroelastic transition point (453 K) a preferential orientation of the displaced Pb(1)-atoms along and Pb(2)-atoms nearly parallel to the twofold axis of the monoclinic phase is realized. Three orientations of the twofold axis with respect to the supergroup are symmetry allowed belonging to three ferroelastic orientation states. The local symmetry of the intermediate regime between 560 K and 453 K is monoclinic, the overall symmetry, however, is trigonal (Joffrin, Benoit, Deschamps and Lambert, 1977; Luspin, Servoin and Gervais, 1979; Salje, Devarajan, Bismayer and Guimaras, 1983; Bismayer, 1990a). The monoclinic signals of the intermediate regime are related to the generation of microdomains with livetimes on the phonon time scale due to the criticality of one order parameter component near 560 K. The intermediate regime is not a phase in the thermodynamic sense but contains dynamical monoclinic clusters on an atomistic length scale.

Pure barium phosphate exhibits no transformation to a ferroelastic phase. First investigations on the critical behaviour of Ba-diluted mixed crystals, $(Pb_{1-x}Ba_x)_3(PO_4)_2$, have been carried out by Bismayer (1990b) and Salje, Bismayer, Wruck and Hensler (1991). For low barium defect concentration a plateau-behaviour of the critical temperature has been discussed. With increasing amount of barium the inhomogeneous local strain leads to space-dependent order parameters described by the Ornstein-Zernike function (Bismayer, 1990b). The result of a defect field in the effective Hamiltonian of the ferroelastic system is a dramatic renormalization of the critical temperature T_c.

Whereas the deformations in the intermediate regime, existing in pure $Pb_3(PO_4)_2$ between 560 K and 453 K, are purely dynamic in character the deformations in doped lead phosphate are static just above T_c (Bismayer, 1990b) and superimposed by reorientational flip motion at higher tempera-

tures. The substitution of lead by barium in $Pb_3(PO_4)_2$ leads to a strong decrease of the spontaneous strain in the ferrophase. A homogeneous transition behaviour of $(Pb_{1-x}Ba_x)_3(PO_4)_2$ has been reported for samples with $0.002 \leq x < 0.07$. However, no detailed information about the crystallographic structure of the mixed crystals, the evolution of the ferroelastic strain with increasing Ba-content and the development of the phase boundary at higher x-values (>0.07) is available so far. Recent investigations by Salje et al. (1991) suggest that for mixed crystals with higher barium content the critical line tends to take infinite negative slope. Therefore, even a small variation in x is expected to result in a large variation of the ferroelastic transition temperature. It will be shown that strain gradients and order parameter fluctuations lead to the spread of T_c over a wide temperature range.

The impact of such inhomogeneous strain distribution on the crystal symmetry and the transition behaviour in highly Ba-diluted lead phosphate has been investigated quantitatively in this work. We focused our investigations especially on the composition $(Pb_{0.92}Ba_{0.08})_3(PO_4)_2$, which shows strong frozen-in order parameter fluctuations and characteristics of non-equilibrium states. The sensitivity on different characteristic length scales of distinct experimental techniques like X-ray or neutron diffraction experiments (ca. 200 Å), optical birefringence measurements (optical wave length) and spectroscopic experiments (some 10 Å) allows us to investigate the macroscopic ferroelastic transformation as well as the variation of the local symmetry in the intermediate regime. It is our aim to present such studies on samples with heterogeneous transition behaviour in this paper. Neutron powder diffraction Rietveld analysis, X-ray diffraction and optical experiments indicate the coexistence of two phases down to 8 K. High-temperature IR spectroscopy reveals the disappearance of monoclinic short-range deformations at ca. 700 K. PDF (probability density function) maps in the paraphase suggest static Pb/Ba disorder mainly for Pb(2)-atoms.

Samples and experimental details

Samples with composition $(Pb_{0.92}Ba_{0.08})_3(PO_4)_2$ were synthesized from starting materials PbO (Merck Art. 7401), $(NH_4)H_2PO_4$ (Merck Art. 1126) and $BaCO_3$ (Merck Art. 1713) as reported earlier (Bismayer and Salje, 1981). Single crystals of $(Pb_{0.92}Ba_{0.08})_3(PO_4)_2$ have been prepared by the Czochralski technique and microcrystalline material has been obtained by fast cooling from the melt in a closed platinum crucible. Electron microprobe analysis showed small inhomogeneities in the Ba-distribution of all Czochralski-grown mixed crystals. In some crystal-bowls of 5 mm diameter the Ba-content decreases from the center to the surface by even

Table 1. Parameters of refinement of $(Pb_{0.92}Ba_{0.08})_3(PO_4)_2$

Temperature (instrument)		8 K (D2B)	270 K (D2B)	300 K (MAN1)	700 K (D2B)
R_{wp}		15.37%	13.52%	9.83%	13.60%
R_{exp}		2.07%	3.57%	6.44%	5.94%
Space group		$C2/c + R\bar{3}m$	$C2/c + R\bar{3}m$	$C2/c + R\bar{3}m$	$R\bar{3}m$
Lattice parameters					
monoclinic fraction		71%	66%	64%	0%
	a [Å]	13.82(1)	13.87(1)	13.86(3)	
	b [Å]	5.688(1)	5.644(1)	5.624(2)	
	c [Å]	9.407(8)	9.495(9)	9.49(2)	
	β [°]	102.34(8)	102.62(7)	102.73(18)	
Pb(1)	x	0.0	0.0	0.0	
	y	0.279(2)	0.274(2)	0.277(4)	
	z	0.25	0.25	0.25	
	B [Å^2]	0.7(2)	1.3(2)	0.4(3)	
Pb(2)	x	0.3189(6)	0.3198(7)	0.318(1)	
	y	0.312(1)	0.305(1)	0.300(2)	
	z	0.3471(7)	0.3506(9)	0.352(2)	
	B [Å^2]	1.1(1)	1.9(2)	1.8(3)	
P	x	0.610(1)	0.5985(5)	0.602(2)	
	y	0.265(3)	0.275(2)	0.275(4)	
	z	0.446(1)	0.451(1)	0.447(2)	
	B [Å^2]	0.5(2)	1.0(2)	1.4(4)	
O(1)	x	0.645(1)	0.6389(9)	0.640(2)	
	y	0.032(2)	0.037(2)	0.030(3)	
	z	0.383(1)	0.386(1)	0.391(3)	
	B [Å^2]	1.4(2)	1.5(3)	0.7(5)	
O(2)	x	0.639(1)	0.650(1)	0.646(3)	
	y	0.508(3)	0.490(2)	0.490(5)	
	z	0.365(1)	0.381(2)	0.379(3)	
	B [Å^2]	2.6(3)	1.4(2)	1.0(4)	
O(3)	x	0.651(1)	0.651(1)	0.643(2)	
	y	0.281(2)	0.272(2)	0.277(3)	
	z	0.612(1)	0.611(1)	0.611(2)	
	B [Å^2]	2.0(2)	1.6(2)	0.4(3)	
O(4)	x	0.4875(6)	0.4893(5)	0.488(1)	
	y	0.245(2)	0.249(2)	0.243(4)	
	z	0.4166(8)	0.4125(9)	0.412(2)	
	B [Å^2]	−0.1(1)	0.1(2)	0.3(3)	
Rhomb. fraction (hexagonal setting)		29%	34%	36%	100%
	a [Å]	5.547(1)	5.555(1)	5.547(4)	5.577(1)
	c [Å]	20.371(2)	20.446(2)	20.380(6)	20.530(1)
Pb(1)	x	0.0	0.0	0.0	0.0
	y	0.0	0.0	0.0	0.0
	z	0.0	0.0	0.0	0.0
	B [Å^2]	3.0(2)	2.5(2)	3.4(4)	3.02(9)

Table 1. (Continued)

Temperature (instrument)		8 K (D2B)	270 K (D2B)	300 K (MAN1)	700 K (D2B)
R_{wp}		15.37%	13.52%	9.83%	13.60%
R_{exp}		2.07%	3.57%	6.44%	5.94%
Space group		$C2/c + R\bar{3}m$	$C2/c + R\bar{3}m$	$C2/c + R\bar{3}m$	$R\bar{3}m$
Pb(2)	x	0.0	0.0	0.0	0.0
	y	0.0	0.0	0.0	0.0
	z	0.216(1)	0.2151(4)	0.2154(8)	0.2131(2)
	B [Å^2]	6.4(3)	4.7(2)	5.2(4)	4.41(8)
	C111				0.024(10)
P	x	0.0	0.0	0.0	0.0
	y	0.0	0.0	0.0	0.0
	z	0.3992(5)	0.4021(6)	0.4011(9)	0.3970(5)
	B [Å^2]	1.4(2)	0.8(2)	0.4(3)	0.81(8)
O(1)	x	0.0	0.0	0.0	0.0
	y	0.0	0.0	0.0	0.0
	z	0.3297(5)	0.3275(5)	0.3289(8)	0.3255(4)
	B [Å^2]	1.6(2)	1.5(2)	2.0(4)	3.33(9)
	C111				0.038(13)
O(2)	x	−0.1504(5)	−0.1515(5)	−0.1501(8)	−0.1484(3)
	y	0.1504(5)	0.1515(5)	0.1501(8)	0.1484(3)
	z	0.4282(3)	0.4276(3)	0.4281(5)	0.4288(2)
	B [Å^2]	2.0(2)	0.9(1)	1.7(2)	2.55(9)

1.5 mol% per 1 mm. In powder samples cooled from the melt with 400 K per hour inhomogeneities could not be detected within the resolution of the microprobe (± 0.2 mol% Ba, lateral 1 μm) and therefore, such a sample was used for the neutron scattering experiments.

The neutron powder diffraction measurements at temperatures 8 K, 270 K and 700 K were carried out at the high-resolution neutron powder diffractometer D2B of the ILL/Grenoble using a wavelength of 1.594 Å from a vertically focusing Ge(335) monochromator. The low-temperature measurement was made by using a standard ILL orange cryostat. For the heating experiments a mirror furnace with Pt sample holder was used (Lorenz, 1988). In the refinement the Pt-lines have been excluded. A preliminary room-temperature measurement on the same sample was made with the neutron powder diffractometer MAN1 at the FRM in Garching with incident wavelength 1.075 Å using a Cu(220) monochromator. As can be seen from Table 1 below, the estimated standard deviations of the parameters refined from the MAN1 data are worse by a factor of two, roughly, in spite of the considerably worse resolution and lower intensity of this instrument as compared to D2B. This is due to a better description of the line shape (Gaussian) in case of MAN1, or, in other words the (known)

non-ideal line shape at D2B is responsible for the rather large goodness of fit (see R_{wp}/R_{exp}) obtained for this instrument. The neutron diffraction data were analyzed with a standard multiphase Rietveld program (Thomas and Bendall, 1978) extended to include anharmonic temperature factors which are calculated via a Gram-Charlier formalism up to the fourth order (Boysen, 1990). To compute joint PDF maps (propability density functions) the powder results were used as input to the program package PROMETHEUS (Zucker et al., 1983).

The measurement of the linear optical birefringence was made from 20 K to 125 K using the rotating analyzer method described by Wood and Glazer (1980) and Bismayer, Salje, Glazer and Cosier (1986). Crystal plates of approximately $1 \times 1 \times 0.2$ mm with large $(100)_{mon}$-planes were investigated by observing monochromatic light ($\lambda = 589.3$ nm) transmitted through a system consisting of a polarizer, a $\lambda/4$ plate, the specimen and an analyzer rotating at constant frequency. The intensity signal which is then independent of the domain orientation was detected using a lock-in system. A continuous-flow He-cryostat was used for optical low-temperature experiments.

High-temperature infrared absorption spectra were recorded between room-temperature and 870 K using a commercial Fourier-transform IR spectrometer (Bruker 113v). A Czochralski grown crystal of $(Pb_{0.92}Ba_{0.08})_3(PO_4)_2$ was crushed and milled using a spex-mill (micro mill, 35 min). IR spectra were obtained by using the standard KBr-pellet technique. The spectra were recorded under vacuum and the pellet was heated in a small temperature controlled furnace.

The spontaneous strain at low temperatures was calculated from the lattice parameters deduced from X-ray powder diffraction patterns which were made by using a modified Huber Guinier Diffractometer System 600 (Abriel and Bismayer, 1989). X-ray powder diagrams were recorded between 12 K and 550 K.

Results

Spontaneous strain

As the global symmetry reduction is $R\bar{3}m \rightarrow C2/c$ the tensor components of the spontaneous strain e_{11}, e_{13} and e_s vanish on approaching T_c from below. Using our own and complementary data from Guimaraes (1979) ($x = 0$) and Bismayer (1990b) ($x = 0.05$) the spontaneous strain was calculated from the monoclinic lattice parameters according to Toledano et al. (1975)

$$e_{11} = \left(\frac{c}{\sqrt{3}} - b\right)/2b \qquad e_{13} = \frac{c + 3a\cos\beta}{6a\sin\beta} \qquad e_s = (2e_{11}^2 + 2e_{13}^2)^{1/2}.$$

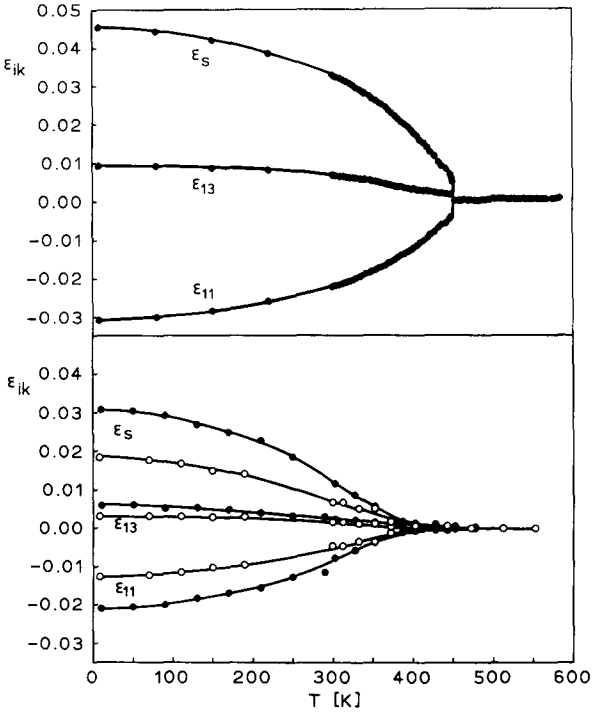

Fig. 1. Spontaneous strain e_{ik} versus temperature measured from powder samples of $(Pb_{1-x}Ba_x)_3(PO_4)_2$ for $x = 0$ (top) and bottom $x = 0.05$ (full circles), $x = 0.08$ (open circles).

The temperature dependence of the strain tensor components is shown in Figure 1 for increasing x-values. The spontaneous strain e_s at 0 K decreases from 0.046 in pure lead phosphate to 0.031 and 0.018 in mixed crystals with 5% and 8% barium. Furthermore, the discontinuous transition in pure $Pb_3(PO_4)_2$ becomes smeared out and a defect tail up to 150 K above T_c is induced which decays proportional to $1/T$ on heating.

Optical birefringence

If a high symmetry orientation for the propagation light can be found, in which no birefringence exists in the paraelastic phase and where an optical birefringence due to the ferroelastic effect occurs in the ferroelastic phase, the birefringence is then called the morphic birefringence. The morphic birefringence follows the spontaneous strain via the elastooptic effect and is, therefore, a sensible measure for the ferroelastic instability. Above the

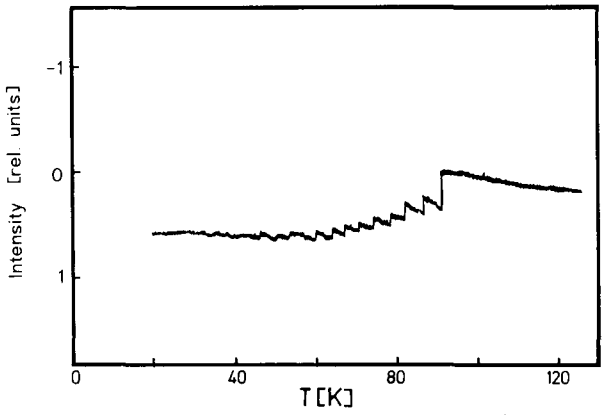

Fig. 2. Rotating analyzer signal output versus temperature (single crystal $x = 0.09$). Above 92 K the crystal is optically isotropic along triad. Between 20 K and 92 K the monoclinic signals of ferroelastic domains disappear discontinuously on heating. The intensity variation above 92 K is an experimental artifact (change of window transparancy in the He-cryostat).

ferroelastic transition point of lead barium phosphate the linear birefringence is zero if the propagation direction of the transmitted light is parallel to the triad of the rhombohedral crystal. Czochralski-grown single crystals with $x = 0.08$ show at room-temperature fully extinct areas next to regions with very small optical birefringence. This pattern displays the optical behaviour of a spatially heterogeneous crystal with the macroscopic ferroelastic transition near room-temperature.

An excellent example of pronounced heterogeneities is the material $(Pb_{0.91}Ba_{0.09})_3(PO_4)_2$. In an area of 2 μm diameter which is homogeneously extinct at 300 K a staircase-like variation of the intensity signal was observed on cooling using the rotating analyzer technique (Fig. 2). The signal corresponds to the integrated intensity transmitted through the region which transforms into the monoclinic phase. No uniform transformation was observed but an increasing number of ferroelastic domains of different orientations in the area under investigation occurs stepwise in the temperature range between 50 K and 92 K. The coexistence of monoclinic and rhombohedral symmetry at low temperatures was found on the optical length scale in all Czochralski-grown mixed crystals with a barium content of $0.075 \leq x \leq 0.105$.

The observation of the birefringence of Ba-diluted lead phosphate crystals over a period of about one year shows furthermore that rhombohedral areas with a barium content of $x = 0.08$ become monoclinic. Small monoclinic ferroelastic domains are formed in a rhombohedral matrix.

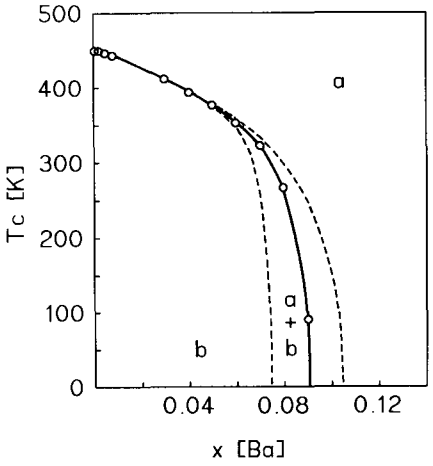

Fig. 3. Dependence of the transition temperature of $(Pb_{1-x}Ba_x)_3(PO_4)_2$ on the Ba-content (from Salje et al., 1991). A coexistence regime of monoclinic and rhombohedral symmetry occurs for $x > 0.075$ (a = $R\bar{3}m$, b = $C2/c$).

Neutron powder diffraction

Although from microprobe analysis chemical variations could only be detected in single crystals inhomogeneity features on a shorter length scale could also exist in the fast cooled powder samples.

As shown below, the structure analysis from neutron powder diffraction measurements reveals the coexistence of both phases with space groups $C2/c$ and $R\bar{3}m$ between 8 K and room-temperature. In a 50 g powder sample with composition $(Pb_{0.92}Ba_{0.08})_3(PO_4)_2$ the absolute content of monoclinic phase is 71% at 8 K and decreases to 66% at 270 K. At 700 K no monoclinic phase could be detected. Taking into account the results from Salje et al. (1991) who measured the critical temperatures by optical birefringence techniques the phase diagram with a coexistence regime of both phases is sketched in Figure 3.

The results of the Rietveld refinements are summarized in Table 1. Observed and calculated profile intensities are shown in Figure 4[1]. At 700 K a satisfactory fit was obtained with space group $R\bar{3}m$ only. The weighted-profile R-factor (R_{wp}) could be reduced from 14.2% to 13.6% by going from harmonic to anharmonic temperature factors. From the anharmonic expansion coefficients (3rd and 4th order) only the parameters C111 of Pb(2) and O(1) proved to be significant (for a discussion of significance of anharmonic thermal parameters from powder patterns see Boysen (1992)). The corresponding PDF maps are shown in Figure 5.

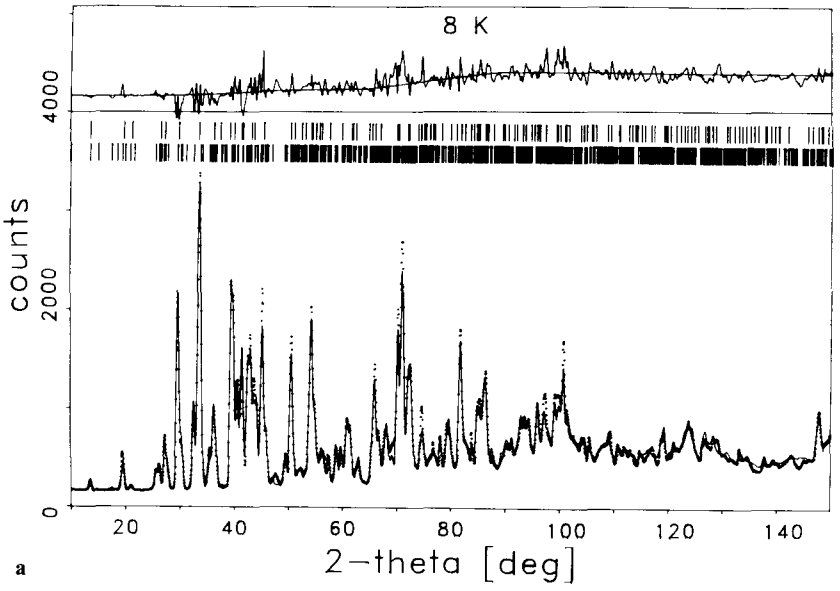
8 K
4000
2000
0
counts
20
40
60
80
100
120
140
2−theta [deg]

a

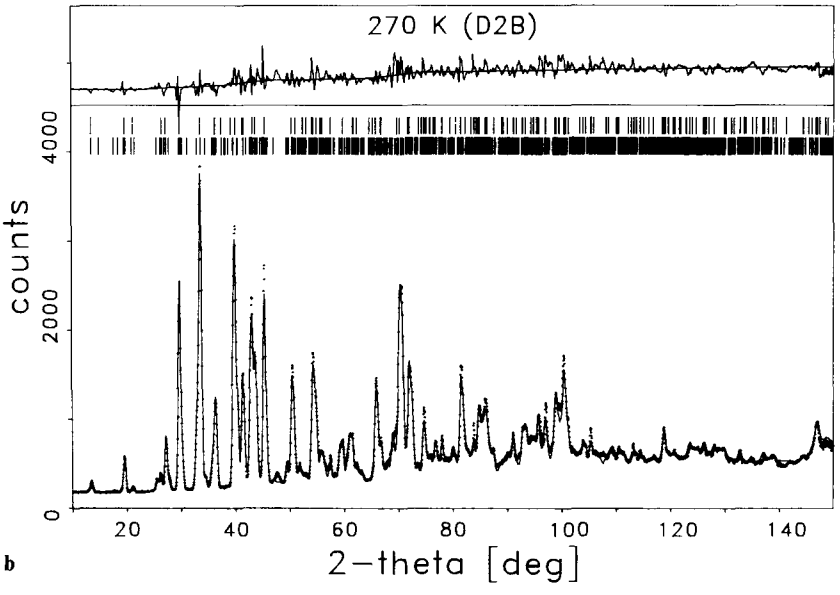
270 K (D2B)
4000
2000
0
counts
20
40
60
80
100
120
140
2−theta [deg]

b

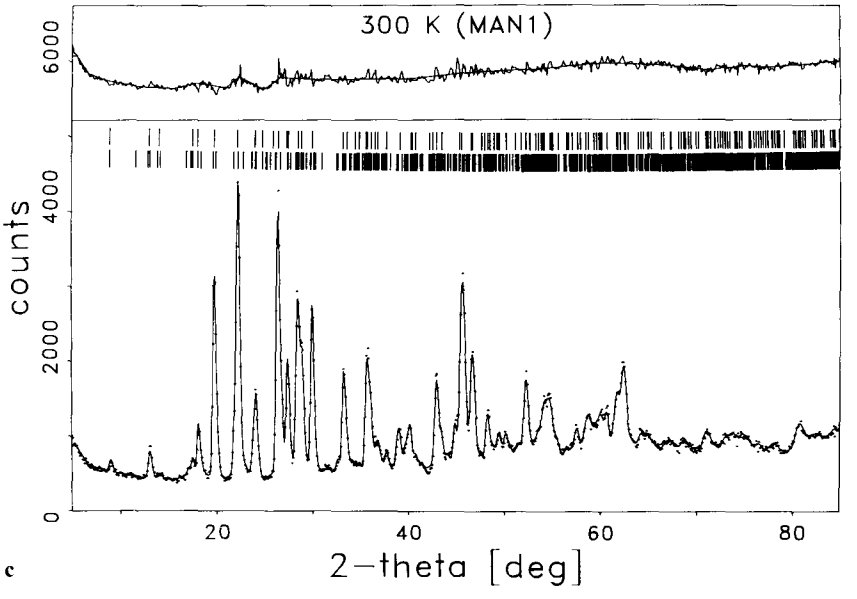

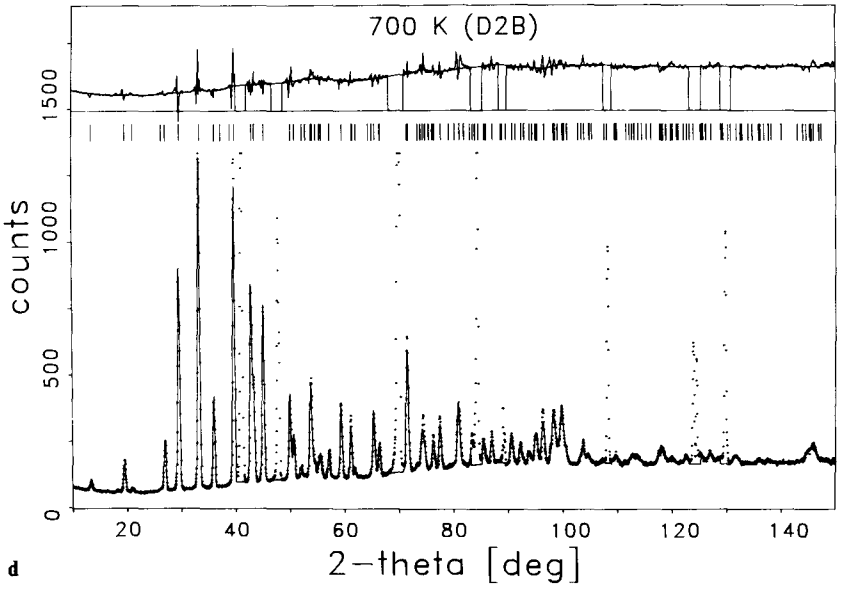

Fig. 4. Observed and calculated neutron powder pattern of $(Pb_{0.92}Ba_{0.08})_3(PO_4)_2$ at (a) 8 K, (b) 270 K, (c) 300 K (MAN1) and (d) 700 K. Difference plots are shown above. Pt-reflexions are excluded from the fit at 700 K.

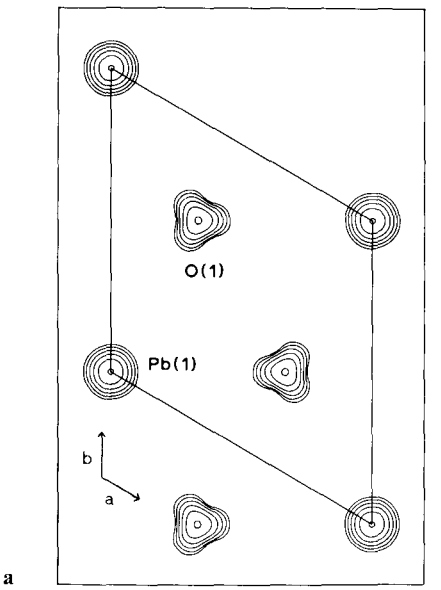

a

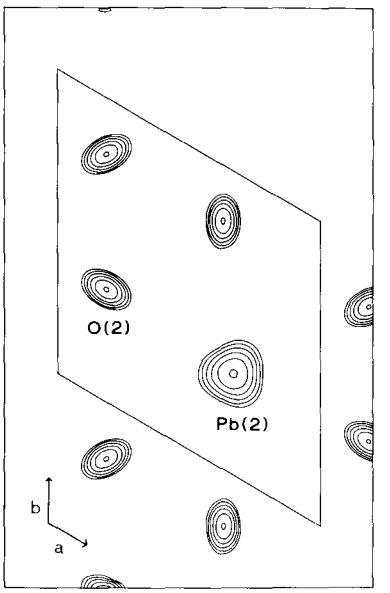

b

Fig. 5. PDF-maps (sections indicated in Fig. 9) of (a) Pb(1) and O(1) $z = 0.0$ and (b) Pb(2) and O(2) at $z = 0.103$ of $(Pb_{0.92}Ba_{0.08})_3(PO_4)_2$ at 700 K. Contour lines correspond to 3%, 6%, 12%, 24%, 48% and 96% of maximum.

At lower temperatures no satisfying fit could be obtained with a single monoclinic phase ($C2/c$) or by a number of other structure models on the basis of subgroups of $R\bar{3}m$ and $C2/c$. Moreover, using a single phase the half-widths of the powder lines increased drastically as compared to the values at 700 K. Instead, the simultaneous refinement of two phases, $C2/c$ and $R\bar{3}m$ with isotropic temperature factors gave reasonable fits. Note that the superposition of the $R\bar{3}m$ and $C2/c$ lines is so close (see Fig. 4[1]) that no clear single $R\bar{3}m$ line can be discerned directly in the diagram. Nevertheless, we have confidence in the results because of the ready convergence of the refinement with reasonable half width parameters and lattice constants as well as the drastic decrease of the R-factor compared with single phase refinements. In a further step anisotropic temperature factors were used. They were, however, not always positive definite. Therefore, only isotropic B-values are given in Table 1.

Due to the severely overlapping diffraction signals of both phases and the large number of parameters no attempts have been made to include anharmonic atomic displacement parameters or a split atom model at room-temperature and below which could eventually have revealed the flip motion in the trigonal phase. A statistical occupation of Pb/Ba on both Pb(1) and Pb(2) positions was used in the refinement. The R-factors (see Table 1) are not fully satisfactory for the D2B data (especially at 8 K). As anticipated before, this is partly due to the non-ideal line shapes at this instrument. Although the two phase fit gave "reasonable" half width parameters, the lines are still broadened as compared to instrumental resolution. A rough analysis of the angular dependence of this broadening in terms of particle sizes and (micro-)strains yielded no unambiguous quantitative results. Nevertheless, there are indications that, at least qualitatively, there is a strain component which is most pronounced for the monoclinic phase at 8 K. Particle sizes of roughly 500–1000 Å are likely. No attempts have been made to include anisotropic strains and particle sizes although these may be a further reason for the residual deviations (the crystals have a plate like habit). For the same reason preferred orientation corrections have been tested but resulted in no improvement of the fit.

IR spectroscopy

The local behaviour of the order parameter was studied using a short range sensitive method like hard mode infrared spectroscopy (Güttler, Salje and Putnis, 1989; Bismayer, 1990b). The evolution of the IR absorption spectrum between 400 cm^{-1} and 1500 cm^{-1} with temperature for $(Pb_{0.92}Ba_{0.08})_3(PO_4)_2$ is shown in Figure 6. The order parameter trans-

[1] Figure 4 and data can be ordered from U. Bismayer, Institut für Mineralogie, Universität Hannover, Welfengarten 1, 30167 Hannover, FRG.

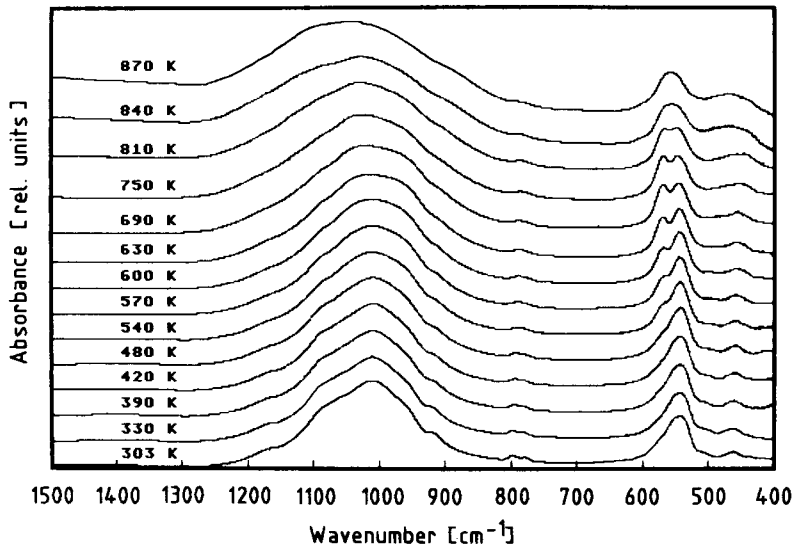

Fig. 6. Temperature evolution of the IR absorption spectrum of $(Pb_{0.92}Ba_{0.08})_3(PO_4)_2$.

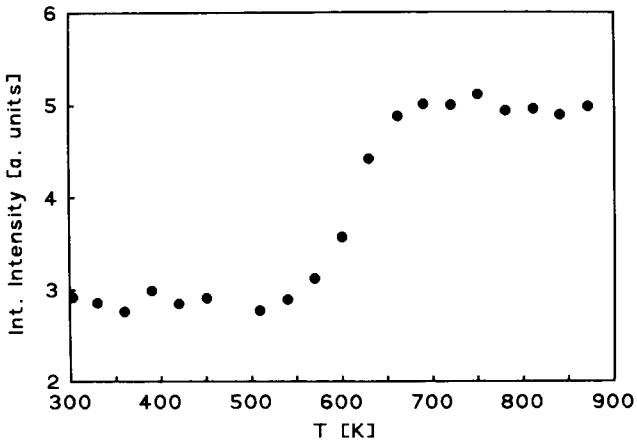

Fig. 7. Integrated IR absorption as a function of temperature for $(Pb_{0.92}Ba_{0.08})_3(PO_4)_2$.

forms according to the A_g representation and, therefore, the lowest order of coupling with infrared active excitations is quadratic according to Bismayer (1990b). In the absorption spectrum of the monoclinic phase near 550 cm^{-1} 3 A_u and 3 B_u-species vibrations are symmetry allowed. They correlate with 1 E_u and 1 A_{2u} mode in the paraelastic phase. Only one A_u and one B_u mode

show strong absorption below T_c and a Least-squares band fit analysis for two bands has been carried out following the procedure described by Bismayer (1990b). The mode near 570 cm^{-1} was found to show the smallest standard deviation (2%). Its integrated intensity increases up to ca. 700 K (Fig. 7). Above 700 K the absorption signal is temperature independent and rhombohedral symmetry is adapted on a local scale.

Discussion

The results reported in this paper show the dependence of structural properties and the change of the ferroelastic transition in Ba-substituted lead phosphate for higher doping levels. These doping levels are equivalent to chemical mixing when Ornstein-Zernike fields overlapp sufficiently so that the defect Gibbs free energy becomes proportional to the square of the order parameter Q (Salje et al., 1991). This results in a linear change of the transition temperature with chemical composition according to

$$T_c^{ex} = T_c - \xi N.$$

T_c is the critical temperature of the defect free crystal, N is the density of impurities and ξ is a coupling constant. It is important to note that the transition temperature is not clearly defined for crystals with Ba-concentrations $0.002 < x < 0.07$ because of the presence of defect tails related to fields conjugate to the order parameter. For those cases Salje et al. (1991) defined T_c^{ex} as the extrapolated value of the critical temperature from the temperature evolution of Q at $T \ll T_c$. At high Ba-concentrations ($x \geq 0.07$) chemical mixing is reached and no tail in the temperature dependence of Q can be observed in single crystals (Fig. 2). T_c^{ex} becomes then identical with the transition temperature of the mixed crystals. However, in powder samples with $x \leq 0.07$ a tail occurs as a consequence of the applied stress during grinding the crystals. Whereas samples with $0.002 \leq x \leq 0.06$ appear homogeneous in their transition behaviour (Salje et al., 1991; Bismayer, 1990b) the material with higher Ba-concentrations shows heterogeneous transformation characteristics. The major effects of the dilution of Pb by large concentrations of Ba in $(Pb_{1-x}Ba_x)_3(PO_4)_3$ are:

1) The linear renormalisation of the critical temperature. For $x \cong 0.1$, T_c is reduced to zero K and the paraelastic phase is stabilized for all mixed crystals with higher Ba-content (Fig. 3).

2) The stability range of the intermediate regime is increased up to 700 K for $x = 0.08$ compared to 560 K in pure lead phosphate (Figs. 6 and 7). Ba-atoms react as pinning centres of the binary axis and hence, static deformations on a local scale appear within this range (Bismayer, 1990b).

3) Condensed fluctuations of the order parameter lead to a two phase regime ($C2/c + R\bar{3}m$) in the phase diagram where the phase boundary shows the highest slope (Fig. 3).

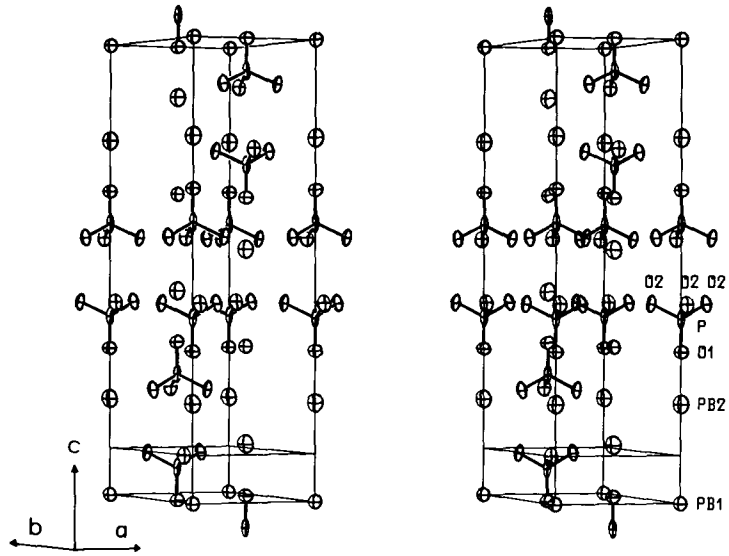

Fig. 8. Crystal structure of $(Pb_{0.92}Ba_{0.08})_3(PO_4)_2$ at 700 K using hexagonal unit cell of the paraelastic phase.

The experimental results of this study allow us to quantify the impact of the Pb/Ba replacement on the structure of the mixed crystals. The crystal structure of $(Pb_{0.92}Ba_{0.08})_3(PO_4)_2$ in its paraelastic phase at 700 K is shown in Figure 8. The topological arrangement resembles that of pure lead phosphate above 560 K.

PDF maps at $z = 0.0$ and 0.103 are shown in Figure 5a and 5b (Figure 8 shows the location of these sections). Whereas Pb(1)-atoms are fully isotropic the PDF-map of Pb(2)-atoms shows three lobes pointing between O(2)-atoms. Possibly these lobes indicate static disorder of displaced Pb(2)/Ba-atoms averaged over a larger number of unit cells. However, from infrared spectroscopy we can deduce the transformation point to the high-temperature phase on a local scale (Salje, Güttler and Ormerod, 1989; Bismayer 1990b). In $(Pb_{0.92}Ba_{0.08})_3(PO_4)_2$ the transition temperature to rhombohedral symmetry is close to 700 K (Fig. 7). Therefore, a more likely explanation for the lobes is of dynamic origin and may be the onset of the symmetry breaking critical behaviour of the displacive mechanism corresponding to the Pb/Ba-shifts perpendicular to the threefold inversion axis. However, the observed displacements of Pb(2) in $C2/c$ are roughly tilted by 30 degrees against the lobes in Figure 5. The nearest neighbour of Pb(2) along **c** is the O(1)-atom with distance 2.31 Å. This atom shows similar lobes as Pb(2) (Fig. 5a) possibly indicating a coupled motion. Note

also the anisotropy (Fig. 8) of the O(2) atoms which is in accordance with this motion, if the PO_4-tetrahedron is taken as a rigid unit.

An inhomogeneous Ba-distribution and a strong inhomogeneous transition behaviour was found in Czochralsky-grown single crystals on an optical length scale (ca. 1 μm). In a single crystal with $x = 0.09$ a stepwise transformation $R\bar{3}m \rightarrow C2/c$ below 95 K was found by measuring the optical birefringence along the triad (Fig. 2). In the powder samples, however, inhomogeneities occur on a much shorter length scale. In powder samples fast cooled from the melt our neutron diffraction studies seem to indicate a correlation range (500–1000 Å) possibly associated with the clustering or ordering of Ba-positions. The most striking influence of small variations in x can be seen when the evolution of the phase boundary $C2/c - R\bar{3}m$ is virtually vertical in the phase diagram $Pb_3(PO_4)_2 - Ba_3(PO_4)_2$. This is the case for compositions with $0.07 \leq x \leq 0.105$ (Fig. 3). Chemical mixing leads to a strong dilution of the spontaneous strain e_s. The ferroelastic strain in mixed crystals with $x = 0.08$ decreases to 40% of its value in pure lead phosphate at 0 K. The transition to the rhombohedral phase is smeared out leading to the defect tails shown in Figure 1. The elastic energy within the tail due to the defects can be estimated from the relation

$$E \propto Q \cdot t = \sqrt{(e_s(T)/e_s(0\ \mathrm{K}))} \cdot (T - T_c^{ex})/T_c^{ex}$$

where t is the reduced temperature and T_c^{ex} is the critical temperature extrapolated from lower temperatures. Relative contributions to the elastic energy at 400 K resulting from the defect field are 3% in crystals with $x = 0.05$ and 9% for a Ba-content of $x = 0.08$.

Rietveld analysis of low-temperature neutron powder diffraction data from a sample with composition $(Pb_{0.92}Ba_{0.08})_3(PO_4)_2$ confirmed a superposition of monoclinic and rhombohedral symmetry. The relatively high R-values, i.e. the non-ideal fits are probably due to the following reasons (in addition to those mentioned before): The peaks of the monoclinic phase are more broadened than those of the rhombohedral phase. Inhomogeneous Ba-distribution on a short length scale leads to contributions from the ferroelastic low-temperature phase and the intermediate phase. The ferroelastic transition point is spread over a wide temperature range. In single crystals this range is in the order of 50 K (Fig. 2). Within the intermediate regime, strain gradients can cause the pinning of the flip motion of the binary axis (Salje et al., 1983; Bismayer, 1990b) and hence, static and dynamic monoclinic signals are superimposed (Bismayer 1990a, 1990b). The increasing monoclinic signals with time seen in the birefringence experiments may be assigned to Pb/Ba ordering kinetics or time dependent pinning of lead atoms in the intermediate phase. Exsolution processes on a microscopic scale cannot be excluded, however. Therefore, a single monoclinic phase, as used in the refinements might be an

oversimplification. In fact, a superposition of several phases with different degrees of "monoclinicity" is present. The microstrains deduced from the fit reflect this behaviour. *Anisotropic* broadening of the line profiles could result from grinding of the powder samples. The application of an external field enhances the inhomogeneous strain distribution on a microscopic scale. In samples with $x \cong 0.08$ the external field can be in the order of magnitude of the ferroelastic field at room-temperature. Furthermore, the perfect cleavage of the crystals perpendicular to $[001]_{hex}$ leads to a preferred orientation of crystallites and explains minor errors in some intensities of strong $00l$-reflexions. In any case, the low-temperature structure refinement clearly confirms the superposition of monoclinic and rhombohedral phases with increasing amount of the ferrophase $C2/c$ on cooling (66% at 270 K, 71% at 8 K). Further investigations of the ordering kinetics in the intermediate phase are under way.

Acknowledgements. We thank Dr. B. Güttler for recording the IR spectra. The low-temperature optical birefringence measurements where performed with the help of Dr. A. M. Glazer and J. Cosier, Dept. of Physics, Oxford. The authors acknowledge financial support by DFG and ARC.

References

Abriel, W., Bismayer, U.: Low-temperature X-ray powder diffraction with a modified Guinier diffractometer: piezoelectricity in $Pb_3(AsO_4)_2$. Phase Transitions **15** (1989) 49.

Bismayer, U.: Stepwise ferroelastic phase transition in $Pb_3(P_{1-x}As_xO_{42}$. In: *Ferroelastic and Co-elastic Phase Transitions in Crystals* (Ed. E. Salje), p. 253–267. Cambridge: Cambridge University Press (1990a).

Bismayer, U.: Hard mode raman spectroscopy and its application to ferroelastic and ferroelectric phase transitions. Phase Transitions **27** (1990b) 211–267.

Bismayer, U., Salje, E.: Ferroelastic phases in $Pb_3(PO_4)_2$-$Pb_3(AsO_4)_2$; X-ray and optical experiments. Acta Crystallogr. **A37** (1981) 145.

Bismayer, U., Salje, E., Glazer, A. M., Cosier, J.: Effect of strain-induced order parameter coupling on ferroelastic behaviour of lead phosphate-arsenate. Phase Transitions **6** (1986) 126.

Boysen, H.: Anharmonic Thermal Parameters, Disorder and Phase Transitions in: *Accuracy in Powder Diffraction II*, (E. Prince ed.), in press.

Boysen, H.: Anharmonic temperature factors from powder diagrams. Acta Crystallogr. **A46** (1990) 265.

Güttler, B., Salje, E., Putnis, A.: Structural states of Mg Cordierite III: infrared spectroscopy and the nature of the hexagonal-modulated transition. Phys. Chem. Minerals **16** (1989) 365.

Guimaraes, D. M. C.: Ferroelastic transformations in lead orthophosphate and its structure as a function of temperature. Acta Crystallogr. **A35** (1979) 108–114.

Joffrin, C., Benoit, J. P., Deschamps, L., Lambert, M.: Étude par diffraction et diffusion de rayons X de la transition de phase ferroélastique du phosphate de plomb: $Pb_3(PO_4)_2$. J. Physique **38** (1977) 205–213.

Keppler, U.: Die Struktur der Tieftemperaturform des Bleiphosphates. Z. Kristallogr. **132** (1970) 228–235.

Lorenz, G.: Thesis (1988). Univ. München, Federal Republic of Germany.

Luspin, Y., Servoin, L., Gervais, F.: Critical behavior of polar modes in lead phosphate near the ferroelastic phase transition. J. Phys. Chem. Solids **40** (1979) 661–668.

Salje, E., Bismayer, U., Wruck, B., Hensler, J.: Influence of lattice imperfections on the transition temperatures of structural phase transitions: the plateau effect. Phase Transitions **35** (1991) 61–74.

Salje, E., Devarajan, V.: Potts model and phase transitions in lead phosphate $Pb_3(PO_4)_2$. J. Phys. C.: Solid State Phys. **14** (1981) L1029.

Salje, E., Devarajan, V., Bismayer, U., Guimaraes, D. M. C.: Phase transitions in $Pb_3(P_{1-x}As_xO_4)_2$: influence of the central peak and flip mode on the Raman scattering of hard modes. J. Phys. C.: Solid State Phys. **16** (1983) 5233.

Salje, E., Güttler, B., Ormerod, C.: Determination of the degree of Al, Si order Q_{od} in kinetically disordered albite using Hard Mode Infrared Spectroscopy. Phys. Chem. Minerals **16** (1989) 576.

Thomas, M. W., Bendall, P. J.: A suite of programs for total profile refinement of a number of powder diffraction patterns. Acta Crystallogr. **A34** (1978) 351.

Toledano, J. C., Pateau, L., Primot, J., Aubrée, J., Morin, D.: Étude dilatométrique de la transition ferroélastique de l'orthophosphate de plomb monocristallin. Mat. Res. Bull. **10** (1975) 103.

Wood, I. G., Glazer, A. M.: Ferroelastic phase transition in $BiVO_4$. 1. Birefringence measurements using the rotating-analyzer method. J. Appl. Crystallogr. **13** (1980) 217.

Zucker, U. H., Perenthaler, E., Kuhs, W. F., Bachmann, R., Schulz, H.: PROMETHEUS. A program system for investigation of anharmonic thermal vibrations in crystals. J. Appl. Crystallogr. **16** (1983) 358.